Comparison of Blood Oxygenation and Cerebral Blood Flow Effects in fMRI: Estimation of Relative Oxygen Consumption Change

Seong-Gi Kim, Kâmil Uğurbil

The most widely-used functional magnetic resonance imaging (fMRI) technique is based on the blood oxygenation level dependent (BOLD) effect, which requires at least partial uncoupling between cerebral blood flow (CBF) and oxygen consumption changes during increased mental activity. To compare BOLD and CBF effects during tasking, BOLD and flow-sensitive alternating inversion recovery (FAIR) images were acquired during visual stimulation with red goggles at a frequency of 8 Hz in an interleaved fashion. With the FAIR technique, absolute and relative CBF changes were determined. Relative oxygen consumption changes can be estimated using the BOLD and relative CBF changes. In gray matter areas in the visual cortex, absolute and relative CBF changes in humans during photic stimulation were 31 ± 11 SD ml/100 g tissue/min and 43 ± 16 SD % (n = 12), respectively, while the relative oxygen consumption change was close to zero. These findings agree extremely well with previous results using positron emission tomography. The BOLD signal change is not linearly correlated with the relative CBF increase across subjects and negatively correlates with the oxygen consumption change. Caution should be exercised when interpreting the BOLD percent change as a quantitative index of the CBF change, especially in inter-subject comparisons.

Key words: perfusion; functional mapping; CBF; $CMRO_2$.

INTRODUCTION

Most functional magnetic resonance imaging (fMRI) studies are based on the blood oxygenation level dependent (BOLD) contrast, caused by alterations in local deoxyhemoglobin content (1–3). The basis of the BOLD technique is the fact that deoxyhemoglobin acts as nature's own intravascular paramagnetic contrast agent (1–5). It is thought that neuronal activation leads to an increase in cerebral blood flow (CBF) without a commensurate elevation in cerebral metabolic rate for O_2 ($CMRO_2$) (i.e., oxygen consumption rate). According to positron emission tomography (PET) studies on humans (6, 7), CBF increases during photic and somatosensory stimulation were 50% and 29%, respectively, while $CMRO_2$ increased only 5% during both tasks. This uncoupling between CBF and $CMRO_2$ increases causes a decrease in capillary and venous deoxyhemoglobin concentrations and therefore increases the T_2^*/T_2-weighted MRI signal.

BOLD-based fMRI studies have been successfully conducted during performance of various tasks, suggesting that uncoupling between CBF and $CMRO_2$ is a general phenomenon. Functional sites determined by the BOLD-based fMRI techniques were consistent with those determined by the CBF-based $H_2{}^{15}O$ PET techniques (8–10) and also with well-known functionally active areas such as somatotopy and hemifield (11, 12). For example, BOLD-based fMRI sites during finger and toe movements agreed well with the well-known somatotopic maps (11). This BOLD-based functional neuroimaging opened a new era of visualizing functional activity in the human brain. However, the BOLD signal change caused by the extent of uncoupling between CBF and $CMRO_2$ may not be correlated linearly with the CBF change, which is presumably modulated by neuronal activity (13). Thus, it is difficult to define the relation of BOLD signal and CBF changes quantitatively. Furthermore, uncoupling between CBF and $CMRO_2$ during increased neuronal activity may not be present in all circumstances and in all regions of the brain (14, 15). Roland and coworkers (14) observed complete coupling between CBF and $CMRO_2$ in the prefrontal cortex, frontal eye fields, parietal lobe, and thalamus during mental calculation. Recently Seitz and Roland (15) re-examined CBF and $CMRO_2$ changes during somatosensory stimulation, similar to the task used by Fox and Raichle (6), and found that some, but not all, areas exhibited uncoupling of CBF and $CMRO_2$.

Recently, we have developed a CBF-based fMRI technique, Flow-sensitive alternating inversion recovery (FAIR) (16), which collects two inversion recovery (IR) images, one with a nonslice-selective inversion pulse and the other with a slice-selective inversion pulse, and then subtracts one from the other. Using this technique, relative and absolute CBF changes can be determined. A detailed analysis for a steady state condition was described in a companion article (17).

To compare activation sites determined by oxygenation- and CBF-based techniques, BOLD and FAIR images were acquired during visual stimulation in an interleaved fashion. From measured CBF and BOLD fractional signal changes, relative changes of $CMRO_2$ were estimated, based on various assumptions (e.g., cerebral blood volume and oxygenation level) (18–20), and correlated with the BOLD changes.

MATERIALS AND METHODS

Studies were performed on a 4 T whole body imaging system with a 1.25 m diameter horizontal bore (SISCo.,

MRM 38:59–65 (1997)

From the Center for Magnetic Resonance Research, Department of Radiology, University of Minnesota Medical School, Minneapolis, Minnesota.

Address correspondence to: Seong-Gi Kim, Ph.D., CMRR, University of Minnesota Medical School, 385 East River Road, Minneapolis, MN 55455.

Received April 17, 1996; revised January 3, 1997; accepted January 7, 1997.

This work was supported by NIH grants RR08079, NS32919, and NS32437; a Whitaker Foundation grant; and a Grant-in-Aid from the University of Minnesota.

0740-3194/97 $3.00

Palo Alto, CA/Siemens, Erlangen, Germany) and a head gradient insert operating at a gradient strength of 30 mT/m and a slew rate of 150 T/m/s along all three axes. Healthy volunteers were studied according to the guidelines approved by the institutional review board of the University of Minnesota; informed consent was obtained from all subjects. For RF transmission and detection, a homogeneous quadrature bird-cage coil was used (21). Manual shimming was performed to improve homogeneity before the collection of fMRI data.

In all imaging studies, conventional anatomic images were collected using TurboFLASH with slice-selective inversion (22). Typical imaging parameters were an inversion time (TI) of 1.2 s, an echo time (*TE*) of 4.7 ms, a repetition time (*TR*) of 9.6 ms, a field of view (FOV) of 24×24 cm^2, an in-plane resolution of 0.94×0.94 mm^2, and a slice thickness of 7 mm. In addition, T_1-weighted echo planar images were acquired using an interleaved echo planar imaging (EPI) technique (23). Typical parameters were a *TE* of 8 ms and an in-plane resolution of 1.88×1.88 mm^2.

fMRI was performed in an oblique slice through the calcarine fissure using a single-shot, gradient-echo EPI technique with trapezoid-shaped gradients for the readout direction and blipped gradients for the phase-encoding direction. Typical parameters were a matrix size of 64×64, an FOV of 24×24 cm^2, a slice thickness of 7 mm, and an acquisition time of 30 ms. To maximize signal intensity of the FAIR image, TI was set to 1.4 s, which is the T_1 of gray matter water protons (24). A five-lobe sinc-shaped RF pulse with a pulse length of 4 ms was used for excitation of spins, and flip angles of IR images were 90°. Inversion pulses were hyperbolic secant pulses with a pulse length of 8 ms. The only difference between the two IR images was the slice-selection gradient during the inversion pulse. The thickness of the slice-selective inversion slab was 15–21 mm, and centers of both imaging and inversion slices were positioned at the same location. IR images were acquired with a *TE* of 20 ms.

To compare directly between BOLD- and CBF-based fMRI, BOLD and FAIR images were collected in an interleaved fashion. Image sets were acquired in the following order: slice-selective IR ("ssIR"), BOLD with a *TE* of 20 ms ("BOLD20"), nonslice-selective IR ("nsIR"), and BOLD with a *TE* of 30 ms ("BOLD30"). The two echo times were used to study inflow effects in BOLD images. To investigate parameter effects in percent signal changes, two different imaging conditions were used: one ("Condition I") was that $TR = 1.4$ s for BOLD images, $TR = 2.8$ s for IR images, and flip angles of BOLD excitation pulses = 45°, and the other ("Condition II") was that $TR = 0.4$ s for BOLD images, $TR = 4.2$ s for IR images, and flip angles of BOLD excitation pulses = 33°. Eight subjects were studied at Condition I, while one subject was imaged at Condition II. Three subjects were investigated at both conditions. During fMRI studies, task and control periods alternated; during each period, 10 image sets were acquired. Visual stimulation with a flashing frequency of 8 Hz was performed using red binocular goggles (GRASS instruments, Quincy, MA).

FAIR images were generated by paired subtraction of nsIR from ssIR images on a pixel-by-pixel basis. Functional maps were calculated according to two criteria: (i) The cross-correlation method was used with a boxcar reference wave form (25); only pixels with a statistically significant activation ($P < 0.05$) were included. A cross-correlation value was chosen, based on the number of images used (25); it was set to 0.3 for 50 images. (ii) Regions with less than four contiguous activated pixels were not included in the functional map (26).

Regions of interest (ROI) were chosen in the gray matter area along the calcarine fissure, excluding the sagittal sinus, based on anatomic and FAIR images. An average fractional signal change was calculated by summing the signal differences between control and task periods and then dividing by the sum of the signal intensities during the control period. For this calculation, pixels were chosen in two different ways; one is from *only activated pixels within ROIs*, and the other is from *all pixels* within ROIs.

Since EPI was used for data collection, BOLD effects contributed to ssIR, nsIR, and FAIR images. Relative CBF changes (relCBF) were calculated by taking into account the BOLD effect in nsIR images; relCBF = (1 + fractional signal change of FAIR)/(1 + fractional signal change of nsIR) − 1. Similarly, an inflow component in ssIR images can be separated from BOLD effects; fractional signal change caused only by the inflow effect = (1 + fractional signal change of ssIR)/(1 + fractional signal change of nsIR) − 1. Then, absolute CBF change was calculated (Eq. [8] in the companion paper; 17). Statistical analyses for comparisons of different measurements were performed by using the RS1 program (BBN Software, Cambridge, MA).

Changes of venous oxygenation levels, $\Delta Y/(1 - Y)$, can be determined from BOLD signal changes. According to Ogawa *et al.* (18), fractional signal changes, $\Delta S/S$, of BOLD images can be described as

$$\Delta S/S = A*TE*(1 - Y)*b*(\Delta Y/(1 - Y) - \Delta b/b) \quad [1]$$

where A is a constant, TE is the gradient echo time, Y is the venous blood oxygenation level during the resting condition, and b is the venous blood volume. The constant A depends on many parameters including the main magnetic field, the vessel orientation, and the susceptibility difference between 100% deoxygenated blood and 100% oxygenated blood. Based on simulations with static averaging for low resolution images where the voxel contains many vessels with various orientations, A is 510 at 4 T (18). Y is set to 0.54 based on the measurement of Lai *et al.* using blood susceptibility effects (19). We assumed that $b = 0.03$. The relative blood volume change, $\Delta b/b$, is closely related to CBF change; we assume that, according to PET studies (20), $\Delta b/b = (\Delta CBF/CBF + 1)^{0.38} - 1$ where $\Delta CBF/CBF$ is the relative CBF change. $\Delta S/S$ was obtained from the nsIR images with a *TE* of 20 ms and the BOLD images with a *TE* of 30 ms.

Using the conservation of matter (Fick's principle), relative change of $CMRo_2$ in tissue, $\Delta CMRo_2/CMRo_2$, can

be determined from the relative changes of both CBF and oxygenation level in venous vessels. Their relationship is

$$\text{relCMRo}_2 = \Delta\text{CMRo}_2/\text{CMRo}_2 = (\Delta\text{CBF/CBF} + 1)(1 - \Delta Y/(1 - Y)) - 1 \quad [2]$$

where relCMRo_2 is the relative CMRo_2 change. (i.e., relative oxygen consumption change) (18). With both relCBF obtained from FAIR and $\Delta Y/(1 - Y)$ estimated using Eq. [1], relCMRo_2 was determined.

RESULTS

A representative fMRI study of visual stimulation is shown in Fig. 1. In the high resolution T_1-weighted anatomic image (Fig. 1A), white matter areas appear bright because an inversion time of 1.2 s was used. Functional maps of ssIR (Fig. 1B), BOLD30 (Fig. 1C), and FAIR (Fig. 1D) were overlaid on the corresponding MR images. Activation is mainly located in the gray matter within the primary visual area along the calcarine fissure, and the sites of activation are consistent in all three fMRI maps. In all 28 fMRI experiments performed by 12 subjects

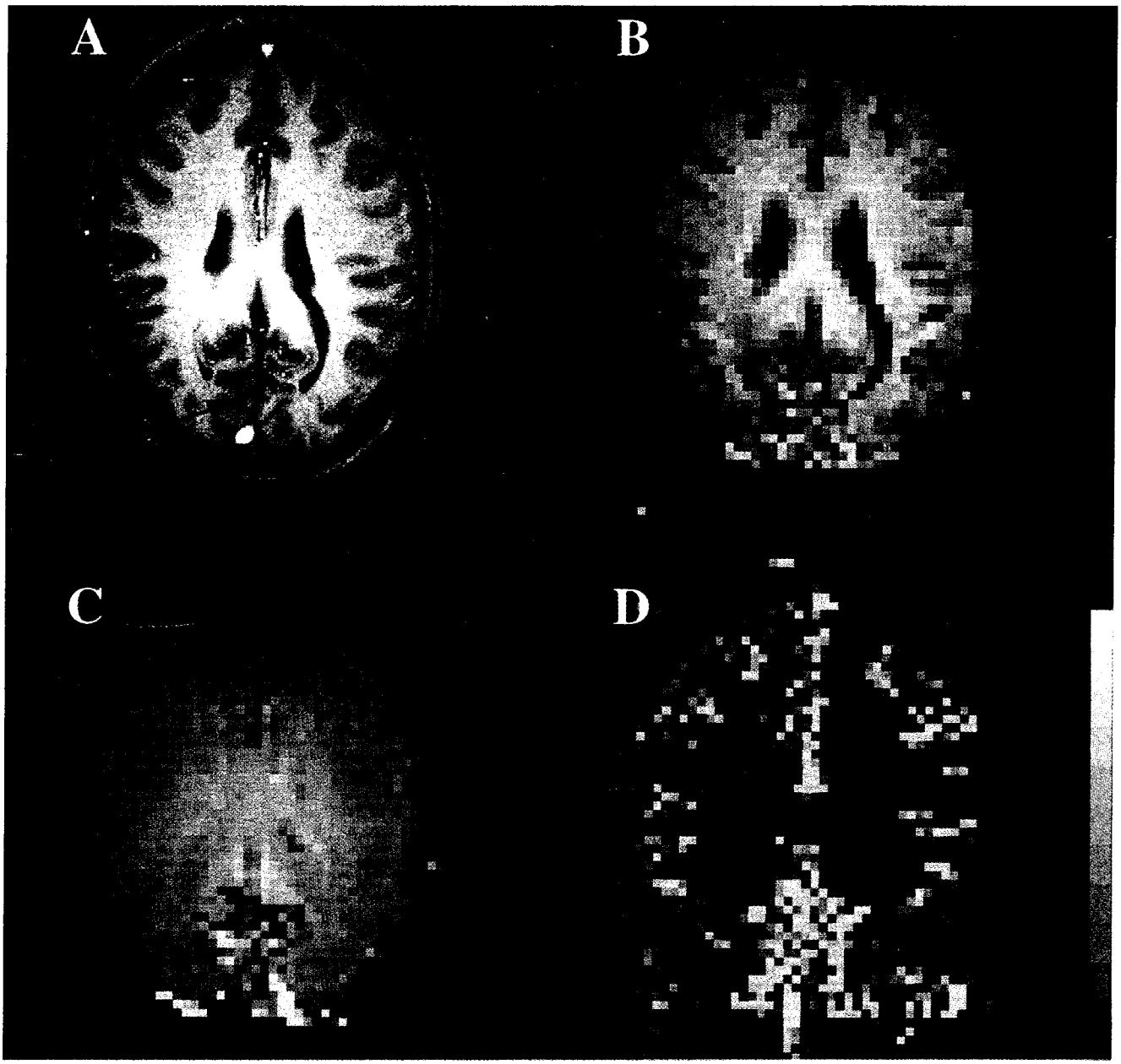

FIG. 1. A representative fMRI study using visual stimulation. A high resolution T_1-weighted TurboFLASH image (A) in an oblique slice along the calcarine fissure is shown. The arrow indicates the primary visual area. Functional maps of ssIR (B), BOLD (C), and FAIR (D) are overlaid on ssIR, BOLD, and FAIR images, respectively. In the color bar, signal change starts at 1% and is incremented by 1% for each color in both BOLD and IR maps, while that starts at 10% and is incremented by 10% for each color in the FAIR map. Percent signal changes were calculated in pixels that were statistically significant ($P < 0.05$).

Table 1
Numbers of Average Activated Pixels ($P < 0.05$) and Their Average Percent Changes during Visual Stimulation[a]

	ssIR	nsIR	BOLD20[b]	BOLD30	relCBF
No. of pixels	75.4 ± 37.0	50.4 ± 34.5	79.5 ± 34.2	70.9 ± 36.2	44.3 ± 20.5
Change (%)	4.22 ± 0.60	3.68 ± 0.91	3.10 ± 0.54	3.76 ± 0.72	73.8 ± 21.5

[a] Seven male and five female subjects were studied (30.5 ± 6.5 years). All subjects except one repeated studies during the same imaging session. The average of multiple measurements in each subject was used. Means and their standard deviations of 12 subjects' data are shown.
[b] Eleven subjects were averaged and the others used 12 subjects.

during visual stimulation, similar activation patterns were observed in the visual cortex area.

To estimate inflow effects in BOLD images, ratios of BOLD fractional signal changes with gradient echo times of 20 and 30 ms were determined in 26 studies. Ratios of percent signal changes in BOLD20 and BOLD30 images within ROIs are 1.12 ± 0.20 SD (n = 18) in Condition I and 1.24 ± 0.11 SD (n = 8) in Condition II. Although inflow effects in BOLD images acquired at Condition II are not expected because of a long delay between two RF excitation pulses (2.8 s), the ratio of percent signal changes of BOLD30 and BOLD20 is still less than the expected value of 1.5, suggesting that inflow effects contribute in BOLD images acquired with the current parameters.

Since 11 subjects (out of 12) performed multiple fMRI experiments during a single imaging session, the reproducibility was determined by the standard deviation of fractional signal changes divided by the mean fractional signal change; variations of fractional signal changes in ssIR, BOLD30, and relCBF were 12 ± 10, 12 ± 9, and 14 ± 10 SD %, respectively. These findings suggest that fMRI signal change during visual stimulation is quite reproducible in a single imaging session for a single subject. Thus, the average of repeated measurements of a single subject was used in Tables 1 and 2. Quantitative analyses of average *activated pixels* in the gray matter area within the visual cortex are tabulated in Table 1. The number of activated pixels is higher in BOLD than in FAIR images.

To compare with data measured by PET, the average signal change of *all pixels within a ROI* in the visual cortex was determined. Individual subject's data were tabulated in Table 2. Since the nsIR images with a gradient echo time of 20 ms acquired using EPI only contain BOLD effects, they were used to calculate changes of venous oxygenation level and oxygen consumption in Table 2. Although BOLD30 images with a higher BOLD effect may contain inflow effects and hence their analyses may be inaccurate, $\Delta Y/(1 - Y)$ and relCMRo$_2$ using BOLD30 are 26.5 ± 8.0 and 3.9 ± 5.4 SD % (n = 12), which is consistent with those using nsIR. The relative cerebral blood volume change determined from relCBF is 14 ± 5 SD % (n = 12).

To determine the relationships of relCBF, BOLD, and relCMRo$_2$ changes, intra-subject averages with their standard deviations were plotted in Fig. 2. BOLD fractional signal changes were obtained from nsIR with a gradient echo time of 20 ms. Five published data in relCBF and relCMRo$_2$ (measured by PET) were also plotted (7), and their BOLD signals were calculated using Eqs. [1] and [2] with the same assumptions. The correlation coefficient (cc) calculated across all 12 subjects was −0.79 between BOLD and relCMRo$_2$, and no correlation was found between relCBF and BOLD (cc = 0.03) and between relCBF and relCMRo$_2$ (cc = 0.58).

DISCUSSION

Since BOLD and FAIR images were acquired simultaneously in the same experiment, physiological parameters were the same, and thus differences between functional images were solely due to fMRI parameters. In the visual cortex, activation areas were consistent among

Table 2
Numbers of Pixels within the Primary Visual Cortex, Average Percent Signal Changes of ssIR and nsIR, Absolute and Relative CBF Changes, and Changes of Oxygenation Level ($\Delta Y/(1 - Y)$) and Oxygen Consumption Rate (relCMRo$_2$) during Visual Stimulation[a]

Subject	No. Pixels	ssIR (%)	nsIR (%)	CBF (ml/100g/min)	relCBF (%)	$\Delta Y/(1 - Y)$ (%)	relCMRo$_2$ (%)
1	90	2.94	1.61	31.3	41.1	25.4	5.2
2[b]	179	4.26	3.08	27.4	33.3	33.4	−11.2
3[b]	101	2.25	0.88	32.4	36.4	18.7	10.8
4[b]	80	1.79	0.91	21.0	26.1	15.6	6.4
5	87	3.17	1.96	28.5	49.7	30.5	4.1
6[b]	74	3.21	1.20	47.3	43.1	23.1	10.0
7	104	3.88	1.54	55.1	83.2	36.8	15.8
8	83	2.00	1.10	21.3	40.8	21.7	10.3
9	172	3.00	1.70	29.9	50.8	29.0	7.0
10	113	2.31	1.31	20.4	21.5	17.0	0.9
11	135	2.67	1.52	26.6	52.4	28.2	9.4
12	160	3.50	2.32	26.8	34.7	28.5	−3.7
Mean ± SD	115 ± 37	2.92 ± 0.75	1.59 ± 0.63	30.7 ± 10.5	42.8 ± 15.9	25.7 ± 6.6	5.4 ± 7.3

[a] Since all subjects except Subject 1 were studied multiple times, the average data were reported here. Means and their standard deviations of 12 subjects' data are shown.
[b] Thickness of an imaging slice was 5 mm and the others were 7 mm thick.

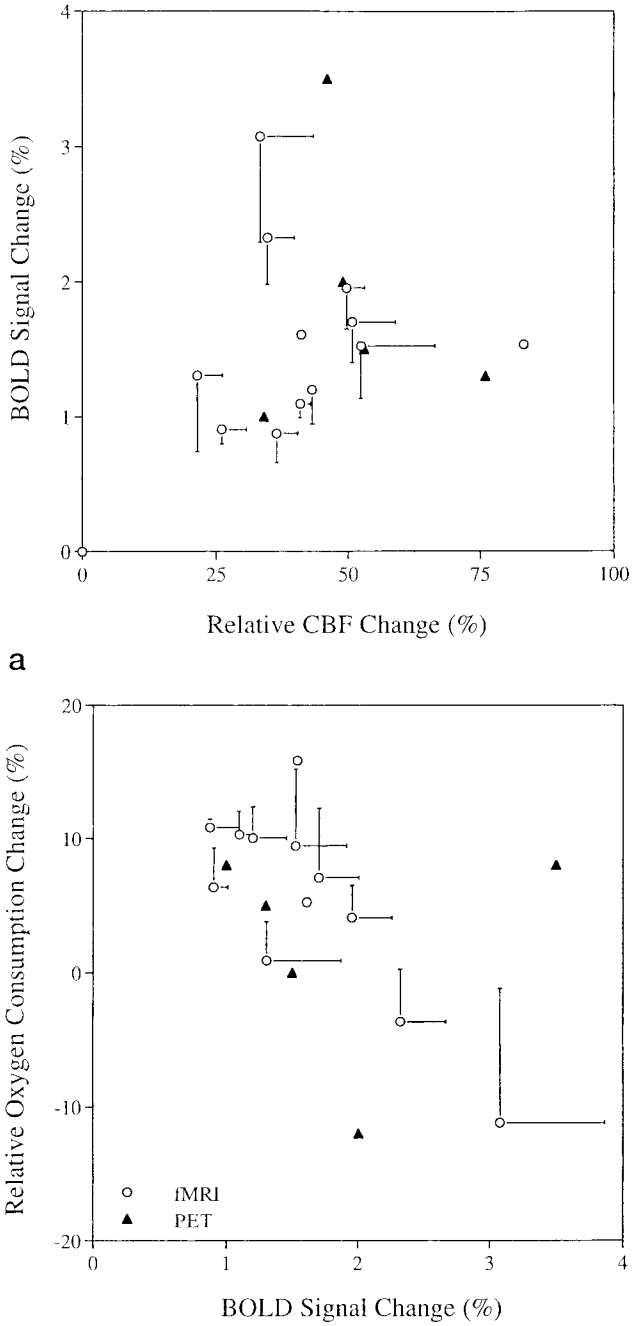

FIG. 2. Relationships of the mean changes of the CBF, BOLD, and $CMRO_2$. BOLD fractional signal changes were obtained from nsIR images. (A) represents the relation between relCBF and BOLD changes, and (B) represents the relationship between BOLD and $relCMRO_2$ changes. Circles and triangles represent fMRI and PET data (7), respectively. Error bars indicate standard deviations of multiple measurements; only one side is shown for clarity.

fMRI maps measured by ssIR, BOLD, and FAIR techniques; areas activated only in the FAIR images were not found (see the companion paper for motor studies; 17). When the same threshold is used to determine fMRI maps, smaller areas of activation were observed in FAIR than in BOLD and ssIR because of the smaller contrast-to-noise ratio of FAIR (17).

The absolute and relative CBF changes of *all pixels within the visual cortex* measured by the FAIR technique during visual stimulation with binocular goggles, 30.7 ± 10.5 SD ml/100 g/min and 43 ± 16 SD % (n = 12), agree well with those measured by PET during the same visual stimulation, 20 ml/100 g/min and 43% (n = 6) (27). Also, the absolute and relative CBF changes measured by the FAIR technique are consistent with the values determined by PET during similar visual stimulation at a frequency of 10 Hz using a reversing red/black checkerboard, 27.1 ± 6.9 SD ml/100 g/min (n = 10, ranging from 16.3 to 40.7 ml/100 g/min) and 50 ± 14 SD % (ranging from 30 to 76%) (7). From relative and absolute CBF changes measured by the FAIR technique, the CBF during the control period can be calculated; the CBF in the gray matter area within the visual cortex is 75 ± 18 SD ml/100 g/min (n = 12), which is consistent with data measured by PET (7, 28, 29), and with values in the companion article (17).

Since the BOLD signal change is dependent on echo time, venous blood volume, venous deoxygenation level, blood volume, and CBF changes, several assumptions were made to quantify venous oxygenation level change and, consequently, $relCMRO_2$ from the BOLD and the relCBF changes. (i) We assumed that the blood volume change during the performance of tasks is related to the relCBF (20). Our calculated value from relCBF in *all* pixels within the visual cortex, 14 ± 5 SD % (n = 12), is similar as the reported value determined by PET, 16% (30). Also, the value in only *activated* pixels within the ROI, 23 ± 5 SD %, is similar to the value determined in activated pixels by MRI with a contrast agent, 32 ± 10 SD % (n = 7), during the same visual stimulation (31). (ii) The venous oxygenation level during the control period was assumed to be 0.54 (19), which was measured at pial venous vessels using high resolution T_2*-weighted images. We expect the oxygenation level to be similar in all levels of the venous vessels, e.g., large veins, venules and venous ends of capillaries. However, arterial ends of capillaries will have higher oxygenation levels, and thus the Y during the control period may be under-estimated. A higher oxygenation level will give a higher $\Delta Y/(1 - Y)$ and smaller $relCMRO_2$ changes. For example, when Y is assumed to be 0.6, $\Delta Y/(1 - Y)$ is 6 ± 2 SD % higher than the current values. (iii) The venous blood volume fraction was assumed to be 3% of tissue. The capillary volume fraction of cat brain is 2.1 ± 0.5 SD % (32), and the average CBV values of monkey brain determined by PET and x-ray fluorescence are 3.5 and 4.7 ml/100 g tissue, respectively (20, 33). Since we expect BOLD signal changes at all venous vessels, including capillaries, the value used here is higher than the capillary volume and less than the total blood volume. When the venous blood volume is assumed to be 2.5%, the resultant $\Delta Y/(1 - Y)$ is 9 ± 2 SD % higher than the current values.

With the aforementioned parameters, oxygenation level change ($\Delta Y/(1 - Y)$) was determined using Eq. [1] with BOLD and relative blood volume changes. The average $\Delta Y/(1 - Y)$ in the visual cortex agrees well with the values in the visual cortex measured by PET (7), 30 ± 8

SD % (n = 5), and in pial veins within the motor cortex during finger opposition determined by MRI, 30% (34). RelCMRo$_2$ change was determined using Eq. [2] with the relCBF and the $\Delta Y/(1 - Y)$; the average relCMRo$_2$ change of the gray matter area in the visual cortex was 5 ± 7 SD %, which agrees well with PET data, −2% (n = 6) (27) and 5 ± 10.3 SD % (n = 5, ranging from −12 to +16%) (7). Using the same assumptions, BOLD signal changes were computed from relCBF and relCMRo$_2$ measured by PET (7); their values agree well with fMRI data (see Fig. 2). This suggests that the parameters used are quite reasonable, or that effects induced by errors of the parameters may compensate each other. Even if errors exist in the determination of relCMRo$_2$, they will be systematic, preserving both the trend of observation and the correlation between different measurements. Nonetheless, the measurement of oxygenation level changes from BOLD with the current model should be validated. A hypercapnia model can be used, in which CBF increases without any oxygen consumption change. In this case, the oxygenation level change determined accurately using Eq. [2] can be compared with the value estimated from BOLD.

Based on *intra-subject* comparison studies with different tasks (8, 35), we expected to see correlation between CBF and BOLD signal changes. For example, higher controlled-force in motor induces higher increases of both CBF and BOLD signals (8). Also, the BOLD signal dependency on visual stimulation frequency agrees well with the CBF dependency measured by PET (35). It should be noted that, if BOLD images contain significant CBF-dependent inflow effects, a strong correlation between CBF and BOLD can be predicted. In this study, the BOLD signal change is not correlated to the relative CBF change *across subjects*. This cannot be explained by techniques since errors due to repeated measurements are generally within 15% of the averages (see Fig. 2A), but may be related to anatomical and physiological differences including vessel architectures (11, 36–40), venous oxygenation levels and oxygen consumption.

In our studies, the calculated oxygen consumption rate was not correlated with the CBF change within the ROI during visual stimulation *across subjects*, supporting the notion that uncoupling between CBF and CMRo$_2$ changes during increased neuronal activity exists. However, we did not determine CMRo$_2$ changes on a pixel-by-pixel basis due to poor contrast-to-noise ratio in a single pixel (17) and large BOLD signal contributions in large vessel areas (11, 36–40). Further investigations are needed to study spatial distributions of CBF and relCMRo$_2$ changes.

Clearly, the BOLD signal change is negatively correlated with the relCMRo$_2$. This correlation can be expected because BOLD is based on uncoupling between CBF and relCMRo$_2$. At a given relCBF, the higher the oxygen consumption rate, the less BOLD signal change will be obtained. Thus, higher BOLD changes do not necessary mean higher CBF changes. Caution should be exercised when interpreting the BOLD percent change as a quantitative index of the CBF change, especially in inter-subject comparisons.

Recent studies suggest that coupling between CBF and CMRo$_2$ is dependent on the nature of the specific stimulus (41). During visual stimulation with a yellow and red checkerboard, reversing at a frequency of 8 Hz, CMRo$_2$ increased significantly in the striate cortex (41). Also, an initial signal decrease in BOLD images has been observed due to CMRo$_2$ increase during visual stimulation with red GRASS goggles (42). The color stimulation may cause extensive activation of cytochrome oxidase blobs, increasing both CMRo$_2$ and CBF. Our observation based on a color stimulation paradigm cannot necessarily be generalized. Further studies are needed, using various tasks, including a black and white stimulus.

CONCLUSION

Activation areas during visual stimulation were consistent among activation maps generated by BOLD, IR and FAIR techniques. Relative and absolute CBF changes, as well as BOLD percent changes, were determined, and the relative oxygen consumption rate was estimated. Relative and absolute CBF and oxygen consumption changes are consistent with previous PET measurements. Furthermore, the BOLD signal change is not correlated with the relative CBF increase during increased neuronal activity due to red/black visual stimulation across subjects.

ACKNOWLEDGMENTS

The authors thank Dr. Seiji Ogawa for stimulating discussion, Dr. Peter Andersen for hardware support, Gregor Adriany for construction of a quadrature birdcage coil, and John Strupp for his processing software (STIMULATE).

REFERENCES

1. S. Ogawa, T.-M. Lee, A. S. Nayak, P. Glynn, Oxygenation-sensitive contrast in magnetic resonance imaging of rodent brain at high magnetic fields. *Magn. Reson. Med.* **14**, 68–78 (1990).
2. S. Ogawa, T.-M. Lee, A. R. Kay, D. W. Tank, Brain magnetic resonance imaging with contrast dependent on blood oxygenation. *Proc. Natl. Acad. Sci. (USA)* **87**, 9868–9872 (1990).
3. S. Ogawa, T.-M. Lee, Magnetic resonance imaging of blood vessels at high fields: in vivo and in vitro measurements and image simulation. *Magn. Reson. Med.* **16**, 9–18 (1990).
4. L. Pauling, C. D. Coryell, The magnetic properties and structure of hemoglobin, oxyhemoglobin, and carbonmonoxyhemoglobin. *Proc. Natl. Acad. Sci. (USA)* **22**, 210–216 (1936).
5. K. R. Thulborn, J. C. Waterton, P. M. Mattews, G. K. Radda, Oxygenation dependence of the transverse relaxation time of water protons in whole blood at high field. *Biochem. Biophys. Acta.* **714**, 265–270 (1982).
6. P. T. Fox, M. E. Raichle, Focal physiological uncoupling of cerebral blood flow and oxidative metabolism during somatosensory stimulation in human subjects. *Proc. Natl. Acad. Sci. (USA)*, **83**, 1140–1144 (1986).
7. P. T. Fox, M. E. Raichle, M. A. Mintun, C. Dence, Nonoxidative glucose consumption during focal physiological neural activity. *Science* **241**, 462–464 (1988).
8. A. Connelly, C. Dettmers, K. M. Stephan, R. Turner, K. J. Friston, R. S. J. Frackowiak, D. G. Gadian, Quantitative comparison of functional magnetic resonance imaging and positron emission tomography using a controlled-force motor paradigm. *in* "Proc., SMR, 3rd Annual Meeting, 1995," p. 786.
9. N. F. Ramsey, B. S. Kirby, P. Van Gelderen, K. F. Berman, J. H. Duyn, J. A. Frank, V. S. Mattay, J. D. van Horn, G. Esposito, C. T. W. Moonen, D. R. Weinberger, Functional mapping of human sensorimotor cortex with 3D BOLD fMRI correlates highly with $H_2{}^{15}O$ PET rCBF. *J. Cereb.*

Blood Flow Metab. **16,** 755–764 (1996).
10. S.-G. Kim, J. J. Sidtis, S. C. Strother, J. R. Anderson, K. Rehm, K. Uğurbil, D. A. Rottenberg, Comparison of functional activation studied by whole brain BOLD- and CBF-based fMRI and [^{15}O]water PET during sequential finger opposition, "Abstracts, Society for Neuroscience, 26th Annual Meeting, 1996," p. 1437.
11. S.-G. Kim, K. Hendrich, X. Hu, H. Merkle, K. Uğurbil, Potential pitfalls of functional MRI using conventional gradient-recalled echo techniques. *NMR Biomed.* **7,** 69–74 (1994).
12. S. Ogawa, D. W. Tank, R. S. Menon, J. M. Ellermann, S.-G. Kim, H. Merkle, K. Uğurbil, Intrinsic signal changes accompanying sensory stimulation: functional brain mapping using MRI. *Proc. Natl. Acad. Sci. (USA)* **89,** 5951–5955 (1992).
13. M. E. Raichle, Circulatory and metabolic correlates of brain functional in normal humans, *in* "Handbook of Physiology - The Nervous System V," American Physiological Society, Bethesda, pp. 643–674, 1987.
14. P. E. Roland, L. Eriksson, S. Stone-Elander, L. Widen, Does mental activity change the oxidative metabolism of the brain? *J. Neurosci.* **7,** 2373–2389 (1987).
15. R. J. Seitz, P. E. Roland, Vibratory stimulation increases and decreases the regional cerebral blood flow and oxidative metabolism: a positron emission tomography (PET) study. *Acta Neurol. Scand.* **86,** 60–67 (1992).
16. S.-G. Kim, Quantification of relative blood flow change by flow-sensitive alternating inversion recovery (FAIR) technique: application to functional mapping. *Magn. Reson. Med.* **34,** 293–301 (1995).
17. S.-G. Kim, N. V. Tsekos, Perfusion imaging by a flow-sensitive alternating inversion recovery (FAIR) technique: application to functional brain imaging. *Magn. Reson. Med.* **37,** 425–435 (1997).
18. S. Ogawa, T. M. Lee, B. Barrere, The sensitivity of magnetic resonance imaging signals of a rat brain to changes in the cerebral venous blood oxygenation. *Magn. Reson. Med.* **29,** 205–210 (1993).
19. S. Lai, E. M. Haacke, W. Lin, D. Chien, D. Levin, In vivo measurement of cerebral blood oxygenation with MRI, *in* "Proc., SMR, 3rd Annual Meeting, 1995," p. 849.
20. R. L. Grubb, Jr., M. E. Raichle, J. O. Eichling, M. M. Ter-Pogossian, The effects of changes in $PaCO_2$ on cerebral blood volume, blood flow, and vascular mean transit time. *Stroke.* **5,** 630–639 (1974).
21. G. Adriany, J. T. Vaughan, P. Andersen, H. Merkle, M. Garwood, K. Uğurbil, Comparison between head volume coils at high fields, *in* "Proc., SMR, 3rd Annual Meeting, 1995," p. 747.
22. A. Haase, Snapshot FLASH MRI: application to T_1-, T_2-, and chemical shift imaging. *Magn. Reson. Med.* **13,** 77–89 (1990).
23. S.-G. Kim, X. Hu, G. Adriany, K. Uğurbil, Fast interleaved echo-planar imaging with navigator: high resolution anatomic and functional images at 4 Tesla. *Magn. Reson. Med.* **35,** 895–902 (1996).
24. S.-G. Kim, X. Hu, K. Uğurbil, Accurate T_1 determination from inversion recovery images: application to human brain at 4 Tesla. *Magn. Reson. Med.* **31,** 445–449 (1994).
25. P. A. Bandettini, A. Jesmanowicz, E. C Wong, J. S. Hyde, Processing strategies for time-course data sets in functional MRI of the human brain. *Magn. Reson. Med.* **30,** 161–173 (1993).
26. S. D. Forman, J. D. Cohen, M. Fitzgerald, W. F. Eddy, M. A. Mintun, D. C. Noll, Improved assessment of significant activation in functional magnetic resonance imaging (fMRI): use of a cluster-size threshold. *Magn. Reson. Med.* **33,** 636–647 (1995).
27. L. Ribeiro, H. Kuwabara, E. Meyer, H. Fujita, S. Marrett, A. Evans, A. Gjedde, Cerebral blood flow and metabolism during nonspecific visual stimulation in normal subjects, in "Quantification of Brain Function. Tracer Kinetics and Image Analysis in Brain PET" (K. Uemura et al., eds.), pp. 229–236, Excerpta Medica, New York, 1993.
28. P. Pantano, J.-C. Baron, P. Lebrun-Grandie, N. Duquesnoy, M.-G. Bousser, D. Comar, Regional cerebral blood flow and oxygen consumption in human aging. *Stroke* **15,** 635–641 (1984).
29. G .L. Lenzi, R. S. J. Frackowiak, T. Jones, J. D. Heather, A. A. Lammertsma, C. G. Rhodes, C. Pozzilli, $CMRo_2$ and CBF by the oxygen-15 inhalation technique. *Eur. Neurol.* **20,** 285–290 (1981).
30. C. T. Gay, S. K. Brannan, P. T. Fox, Human functional brain mapping: functional areas, variables, and information theory, *in* "Diffusion and Perfusion Magnetic Resonance Imaging" (D. Le Bihan, ed.), pp. 217–227, Raven Press, New York, 1995.
31. J. W. Belliveau, D. N. Kennedy, R. C. McKinstry, B. R. Buchbinder, R. M. Weisskoff, M. S. Cohen, J. M. Vevea, T. J. Brady, B. R. Rosen, Functional mapping of the human visual cortex by magnetic resonance imaging. *Science* **254,** 716–719 (1991).
32. G. Pawlik, A. Rackl, R. J. Bing, Quantitative capillary topography and blood flow in the cerebral cortex of cats: an in vivo microscopic study. *Brain Res.* **208,** 35–58, (1981).
33. M. E. Phelps, R. L. Grubb, Jr., M. M. Ter-Pogossian, Correlation between $PaCO_2$ and regional blood volume by x-ray fluorescence. *J. Appl. Physiol.* **35,** 447–475 (1973).
34. S. Lai, M. Haacke, J. R. Reichenbach, K. Kuppusamy, F. Hoogenraad, H. Takeichi, W. Lin, In vivo quantification of brain activation-induced change in cerebral blood oxygen saturation using MRI, *in* "Proc., SMR, 4th Annual Meeting, 1996," p. 1756.
35. K. K. Kwong, J. W. Belliveau, D. A. Chesler, I. E. Goldberg, R. M. Weisskoff, B. P. Poncelet, D. N. Kennedy, B. E. Hoppel, M. S. Cohen, R. Turner, H.-M. Cheng, T. J. Brady, B. R. Rosen, Dynamic magnetic resonance imaging of human brain activity during primary sensory stimulation. *Proc. Natl. Acad. Sci. (USA)* **89,** 5675–5679 (1992).
36. R. S. Menon, S. Ogawa, D. W. Tank, K. Uğurbil, 4 Tesla gradient recalled echo characteristic of photic stimulation-induced signal changes in the human primary visual cortex. *Magn. Reson. Med.* **30,** 380–386 (1993).
37. S. Lai, A. L. Hopkins, E. M. Haacke, D. Li, B. A. Wasserman, P. Buckley, L. Friedman, H. Meltzer, P. Hedera, R. Friedland, Identification of vascular structures as a major source of signal contrast in high resolution 2D and 3D functional activation imaging of the motor cortex at 1.5T: preliminary results. *Magn. Reson. Med.* **30,** 387–392 (1993).
38. J. H. Duyn, C. T. W. Moonen, G. H. van Yperen, R. W. de Boer, P. R. Luyten, Inflow versus deoxyhemoglobin effects in BOLD functional MRI using gradient echoes at 1.5T. *NMR Biomed.* **7,** 4–9 (1994).
39. J. Frahm, K.-D. Merboldt, W. Hanicke, A. Kleinschmidt, H. Boecker, Brain and vein - oxygenation or flow? On signal physiology in functional MRI of human brain activation. *NMR Biomed.* **7,** 45–53 (1994).
40. S. Segebarth, V. Belle, C. Delon, R. Massarelli, J. Decety, J.-F. Le Bas, M. Decorps, A. L. Benabid, Functional MRI of the human brain: predominance of signals from extracerebral veins. *NeuroReport* **5,** 813–816 (1994).
41. M. Vaface, S. Marrett, T. Paus, A. Gjedde, A. C. Evans, A. Ptito, and E. Meyer, Oxidative metabolism in human visual cortex during physiological activation studied by PET, *in* "Abstracts, Society for Neuroscience, 26th Annual Meeting, 1996," p. 1060.
42. R. S. Menon, S. Ogawa, J. S. Strupp, P. Andersen, K. K. Uğurbil, BOLD-based functional MRI at 4 Tesla includes a capillary bed contribution: echo-planar imaging correlates with previous optical imaging using intrinsic signals. *Magn. Reson. Med.* **33,** 453–459 (1995).